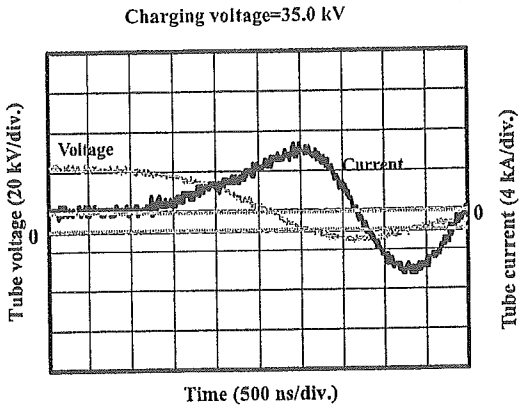

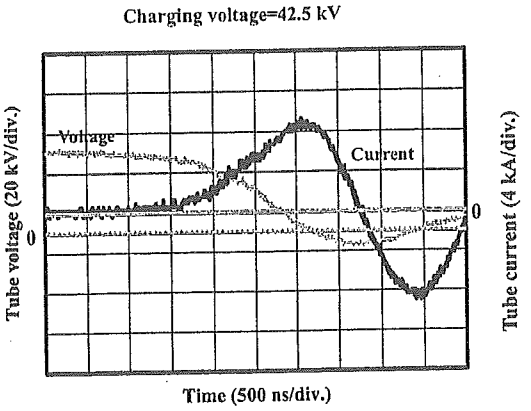

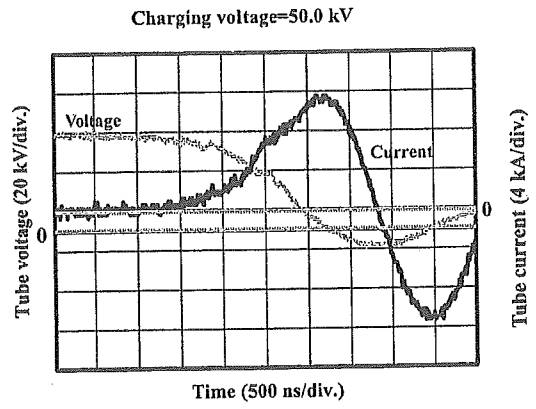

Figure 4: Tube voltages and currents with changing charging voltage.

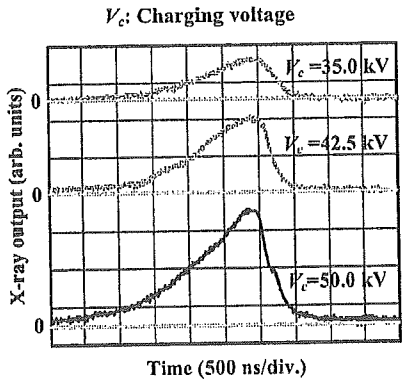

Figure 5: X-ray outputs at indicated conditions.

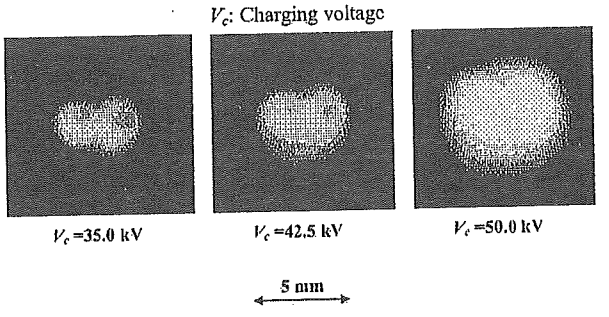

Figure 6: Images of plasma x-ray source of double target.

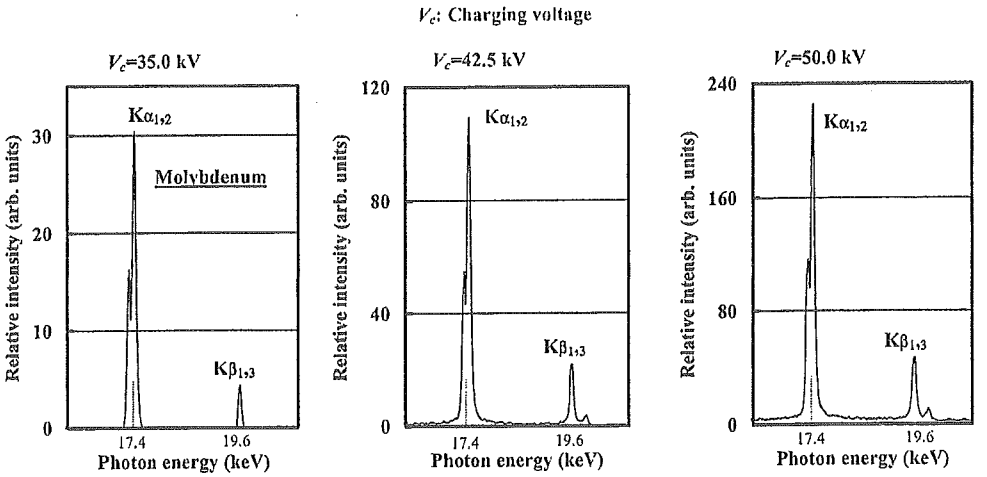

Figure 7: X-ray spectra near molybdenum K-series characteristic x rays.

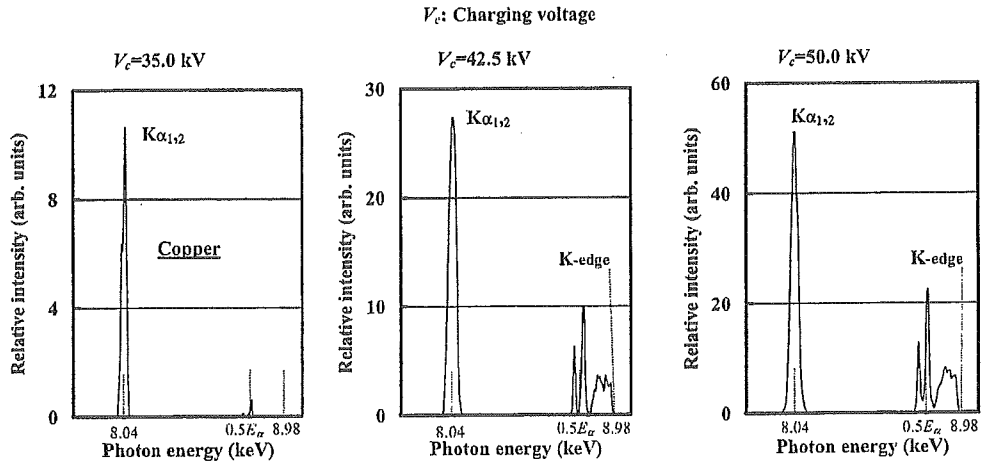

Figure 8: X-ray spectra near copper K-series characteristic x rays.

4. RADIOGRAPHY

The plasma radiography was performed by the CR system (Konica Regius 150) without using a filter, and the distance between the x-ray source and imaging plate was 1.2 m.

Figure 9 shows radiograms of tungsten wires coiled around a pipe made of polymethyl methacrylate with a charging voltage of 45 kV. Although the image contrast increased with increases in the wire diameter, a 50-μm-diameter wire could be observed. Next, the image of water falling into a polypropylene beaker from an glass test tube is shown in Fig. 10. This image was taken with a charging voltage of 50 kV, and an iodine-based contrast medium was added a little. Because the x-ray duration was about 1 μs, the stop-motion image of water was obtained. Figure 11 shows an angiogram of the external ear of a rabbit with a charging voltage (V_c) of 45 kV. In angiography, iodine-based microspheres of 15 μm in diameter were used, and fine blood vessels of about 100 μm are clearly visible. Figures 12 and 13 show angiograms of a rabbit heart (V_c=45 kV) and a thigh (V_c=50 kV), respectively, and fine blood vessels were visible.

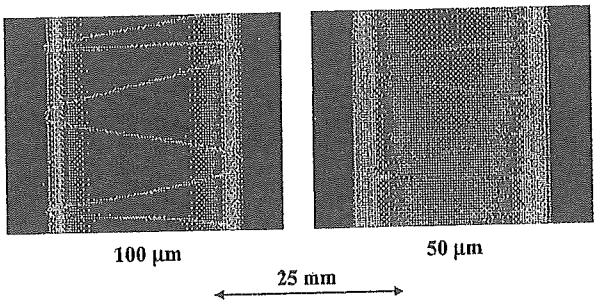

Figure 9: Radiograms of tungsten wires coiled around pipe made of polymethyl methacrylate.

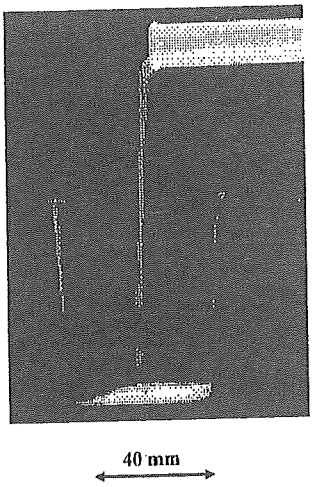

Figure 10: Radiogram of water from glass test tube.

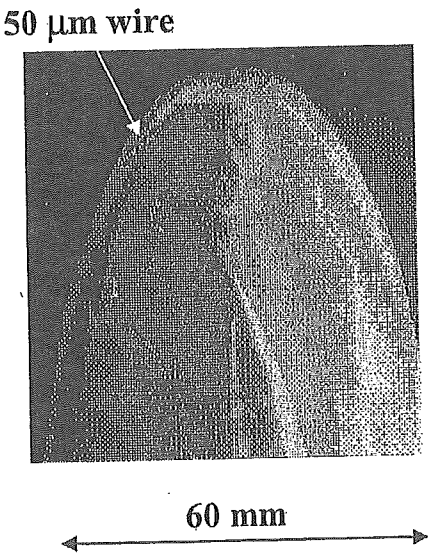

Figure 11: Angiogram of external ear.

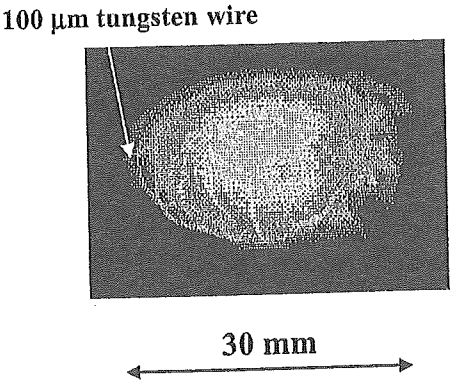

Figure 12: Angiogram of rabbit heart.

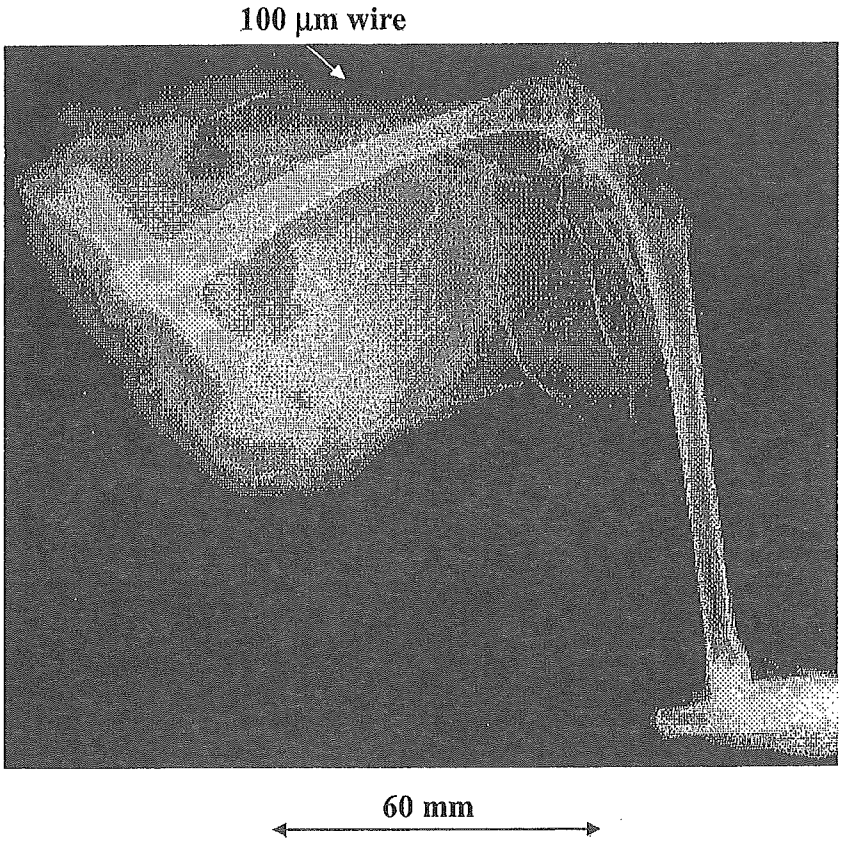

Figure 13: Angiogram of rabbit thigh.

5. DISCUSSION

Regarding the spectrum measurement, although we obtained intense and sharp molybdenum K-series lines, we could not observe copper Kβ lines. In addition, we observed $0.5E_{\alpha}$ lines and the copper K-absorption edge. If we assume that the $0.5E_{\alpha}$ lines are molybdenum Kα lines detected by the high order diffraction, the molybdenum Kβ lines, the copper Kβ lines, and the bremsstrahlung rays should be observed.
In this research, we obtained sufficient characteristic x-ray intensity per pulse for CR radiography without using a monochromatic filter, and the generator produced number of characteristic photons was approximately 4×10^{8} photons/cm^2 at 1.0 m per pulse. In addition, since the photon energy of characteristic x rays can be controlled by changing target elements, various quasi-monochromatic high-speed radiographies, such as flash energy subtraction radiography using a metal filter and wide latitude radiography, will be possible.

ACKNOWLEDGMENT

This work was supported by Grants-in-Aid for Scientific Research (13470154, 13877114, 16591181and 16591222) and Advanced Medical Scientific Research from MECSST, Health and Labor Sciences Research Grants(RAMT-nano-001, RHGTEFB-genome-005 and RHGTEFB-saisei-003), Grants from Keiryo Research Foundation, The Promotion and Mutual Aid Corporation for Private Schools of Japan, Japan Science and Technology Agency (JST), and New Energy and Industrial Technology Development Organization (NEDO, Industrial Technology Research Grant Program in '03).

REFERENCES

1. M. Torikoshi, T. Tsunoo, M. Sasaki, M. Endo, Y. Noda, T. Kohno, K. Hyodo, K. Uesugi and N. Yagi: "Electron density measurement with dual-energy x-ray CT using synchrotron radiation," *Phys. Med. Biol.*, **48**, 673-685, 2003.
2. F. E. Carroll, M. H. Mendenhall, R. H. Traeger, C. Brau and J. W. Waters, "Pulsed tunable monochromatic x-ray beams from a compact source: New opportunities," *Am. J. Roentgenol.*, **181**, 1197-1202, 2003.
3. A. Mattsson, "Some characteristics of a 600 kV flash x-ray tube," *Physica Scripta*, **5**, 99-102, 1972.
4. R. Germer, "X-ray flash techniques," *J. Phys. E: Sci. Instrum.*, **12**, 336-350, 1979.
5. E. Sato, H. Isobe and F. Hoshino, "High intensity flash x-ray apparatus for biomedical radiography," *Rev. Sci. Instrum.*, **57**, 1399-1408, 1986.
6. E. Sato, S. Kimura, S. Kawasaki, H. Isobe, K. Takahashi, Y. Tamakawa and T. Yanagisawa, "Repetitive flash x-ray generator utilizing a simple diode with a new type of energy-selective function," *Rev. Sci. Instrum.*, **61**, 2343-2348, 1990.
7. A. Shikoda, E. Sato, M. Sagae, T. Oizumi, Y. Tamakawa and T. Yanagisawa, "Repetitive flash x-ray generator having a high-durability diode driven by a two-cable-type line pulser," *Rev. Sci. Instrum.*, **65**, 850-856, 1994.
8. E. Sato, K. Takahashi, M. Sagae, S. Kimura, T. Oizumi, Y. Hayasi, Y. Tamakawa and T. Yanagisawa, "Sub-kilohertz flash x-ray generator utilizing a glass-enclosed cold-cathode triode," *Med. & Biol. Eng. & Comput.*, **32**, 289-294, 1994.
9. K. Takahashi, E. Sato, M. Sagae, T. Oizumi, Y. Tamakawa and T. Yanagisawa, "Fundamental study on a long-duration flash x-ray generator with a surface-discharge triode," *Jpn. J. Appl. Phys.*, **33**, 4146-4151, 1994.
10. E. Sato, M. Sagae, E. Tanaka, Y. Hayasi, R. Germer, H. Mori, T. Kawai, T. Ichimaru, S. Sato, K. Takayama and H. Ido: Quasi-monochromatic flash x-ray generator utilizing a disk-cathode molybdenum tube, *Jpn. J. Appl. Phys.*, **43**, 7324-7328, 2004.
11. E. Sato, Y. Hayasi, R. Germer, E. Tanaka, H. Mori, T. Kawai, H. Obara, T. Ichimaru, K. Takayama and H. Ido, "Intense characteristic x-ray irradiation from weakly ionized linear plasma and applications," *Jpn. J. Med. Imag. Inform. Sci.*, **20**, 148-155, 2003.
12. E. Sato, Y. Hayasi, R. Germer, E. Tanaka, H. Mori, T. Kawai, H. Obara, T. Ichimaru, K. Takayama and H. Ido, "Irradiation of intense characteristic x-rays from weakly ionized linear molybdenum plasma," *Jpn. J. Med. Phys.*, **23**, 123-131, 2003.
13. E. Sato, Y. Hayasi, R. Germer, E. Tanaka, H. Mori, T. Kawai, T. Ichimaru, K. Takayama and H. Ido, "Quasi-monochromatic flash x-ray generator utilizing weakly ionized linear copper plasma," *Rev. Sci. Instrum.*, 74, 5236-5240, 2003.
14. E. Sato, R. Germer, Y. Hayasi, Y. Koorikawa, K. Murakami, E. Tanaka, H. Mori, T. Kawai, T. Ichimaru, F. Obata, K. Takahashi, S. Sato, K. Takayama and H. Ido: Weakly ionized plasma flash x-ray generator and its distinctive characteristics. *SPIE*, **5196**, 383-392, 2003.
15. E. Sato, Y. Hayasi, R. Germer, E. Tanaka, H. Mori, T. Kawai, T. Ichimaru, S. Sato, K. Takayama and H. Ido, "Sharp characteristic x-ray irradiation from weakly ionized linear plasma," *J. Electron Spectrosc. Related Phenom.*, **137-140**, 713-720, 2004.
16. E. Sato, K. Sato and Y. Tamakawa, "Film-less computed radiography system for high-speed imaging," *Ann. Rep. Iwate Med. Univ. Sch. Lib. Arts and Sci.*, **35**, 13-23, 2000.

*obara@rad.cms.tohoku.ac.jp; phone +81-22-717-7941; fax +81-22-717-7944

Compact monochromatic flash x-ray generator utilizing a disk-cathode molybdenum tube

Eiichi Sato[a)]
Department of Physics, Iwate Medical University, 3-16-1 Honchodori Morioka 020-0015, Japan

Etsuro Tanaka
Department of Nutritional Science, Faculty of Applied Bio-science, Tokyo University of Agriculture, Setagayaku 156-8502, Japan

Hidezo Mori
Department of Cardiac Physiology, National Cardiovascular Center Research Institute, Osaka 565-8565 Japan

Toshiaki Kawai
Electron Tube Division #2, Hamamatsu Photonics K. K., Iwata-gun 438-0193, Japan

Toshio Ichimaru
Department of Radiological Technology, School of Health Sciences, Hirosaki University, Hirosaki 036-8564, Japan

Shigehiro Sato
Department of Microbiology, School of Medicine, Iwate Medical University, Morioka 020-8505, Japan

Kazuyoshi Takayama
Shock Wave Research Center, Institute of Fluid Science, Tohoku University, Sendai 980-8577, Japan

Hideaki Ido
Department of Applied Physics and Informatics, Faculty of Engineering, Tohoku Gakuin University, Tagajo 985-8537, Japan

(Received 8 April 2004; revised 16 October 2004; accepted for publication 18 October 2004; published 15 December 2004)

The high-voltage condensers in a polarity-inversion two-stage Marx surge generator are charged from −50 to −70 kV by a power supply, and the electric charges in the condensers are discharged to an x-ray tube after closing gap switches in the surge generator with a trigger device. The x-ray tube is a demountable diode, and the turbo molecular pump evacuates air from the tube with a pressure of approximately 1 mPa. Clean molybdenum Kα lines are produced using a 20 μm-thick zirconium filter, since the tube utilizes a disk cathode and a rod target, and bremsstrahlung rays are not emitted in the opposite direction to that of electron acceleration. At a charging voltage of −70 kV, the instantaneous tube voltage and current were 120 kV and 1.0 kA, respectively. The x-ray pulse widths were approximately 70 ns, and the generator produced instantaneous number of Kα photons was approximately 3×10^7 photons/cm^2 per pulse at 0.5 m from the source of 3.0 mm in diameter. © *2005 American Association of Physicists in Medicine.* [DOI: 10.1118/1.1829247]

Key words: x-ray source, x-ray tube, x-ray spectra, rapid imaging, x-ray beam filtration, monochromatic x ray

I. INTRODUCTION

In recent years, many valuable discoveries have been made in laser technology, and soft x-ray lasers of neonlike argon (46.9 nm, 26.4 eV) have been produced using a gas-discharge capillary.[1–3] In these experiments, the laser energy increased with increases in the capillary length, and these kinds of first discharges can generate hot and dense plasma columns with aspect ratios of 1000:1. However, it is difficult to increase the laser photon energy to 10 keV or beyond.

We have developed several different soft flash x-ray generators[4–8] corresponding to specific radiographic objectives, and a major goal in our research is the development of an intense and clean monochromatic x-ray generator that can impact applications with medical radiography. In view of this situation, we confirmed irradiation of intense K-series characteristic x rays from the plasma axial direction by forming weakly ionized linear plasma.[9–12] In the plasma, bremsstrahlung spectra with photon energies of higher than the K-absorption edge are effectively absorbed and are converted into fluorescent x rays, and the plasma then transmits the fluorescent rays easily. However, the bremsstrahlung x rays are produced using a molybdenum target,[11] since high photon energy bremsstrahlung x rays are not absorbed effectively in the linear plasma.

Without forming the linear plasma, because bremsstrahlung rays are not emitted in the opposite direction to that of electron acceleration, characteristic x rays can be produced by considering the angle dependence of bremsstrahlung x rays. As compared with the plasma generator, the photon

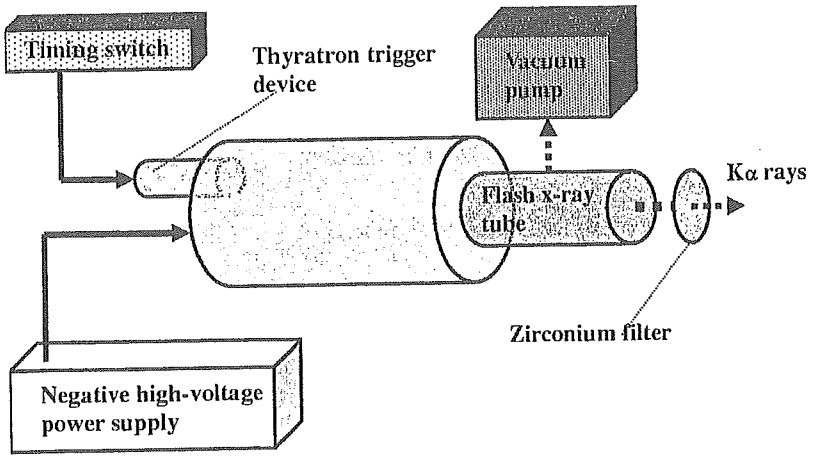

FIG. 1. Block diagram of the compact quasimonochromatic flash x-ray generator with a cold-cathode monochromatic diode.

energy of the characteristic x rays can be increased by increasing the maximum output voltage of the pulse generator, since a multistage Marx generator[13,14] can be employed. In this case, the output voltage is equal to the value of the condenser charging voltage multiplied by the stage number.

In this article, we describe a compact flash x-ray generator utilizing a molybdenum-target radiation tube, used to perform a preliminary experiment for producing clean monochromatic x rays.

II. GENERATOR

A. High-voltage circuit

Figure 1 shows a block diagram of a compact monochromatic flash x-ray generator. This generator consists of the following components: a constant high-voltage power supply, a surge Marx generator with a capacity during main discharge of 425 pF, a thyratron trigger device of the surge generator, a turbo molecular pump, and a flash x-ray tube. Since the electric circuit of the high-voltage pulse generator employs a polarity-inversion two-stage Marx line[13,14] (Fig. 2), the surge generator produces twice the potential of the condenser charging voltage. When two condensers inside of the surge generator are charged from −50 to −70 kV, the ideal output voltage ranges from 100 to 140 kV.

B. X-ray tube

The x-ray tube is a demountable diode type, as illustrated in Fig. 3. This tube is connected to the turbo molecular pump with a pressure of about 1 mPa and consists of the following major devices: a rod-shaped molybdenum target 3.0 mm in diameter, a disk cathode made of graphite, a polyethylene terephthalate (Mylar) x-ray window 0.25 mm in thickness, and a polymethyl methacrylate tube body. The target-cathode space was regulated to 1.0 mm from the outside of the x-ray tube by rotating the anode rod, and the transmission x rays are obtained through a 1.0 mm-thick graphite cathode and an x-ray window. Because bremsstrahlung rays are not emitted in the opposite direction to that of electron acceleration (Fig. 4), molybdenum Kα rays can be produced using a 20 μm-thick zirconium K-edge filter.

III. CHARACTERISTICS

A. Tube voltage and current

Tube voltage and current were measured by a high-voltage divider with an input impedance of 10 kΩ and a current transformer, respectively (Fig. 5). The voltage and current displayed roughly damped oscillations because the discharge resistance in the tube varied rapidly from infinity

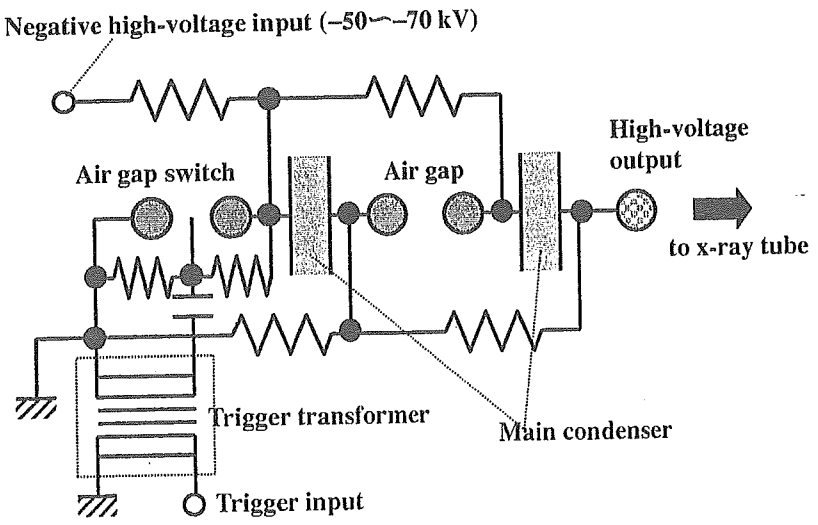

FIG. 2. Circuit diagram of the two-stage surge Marx generator. The generator produces twice the potential of the condenser charging voltage.

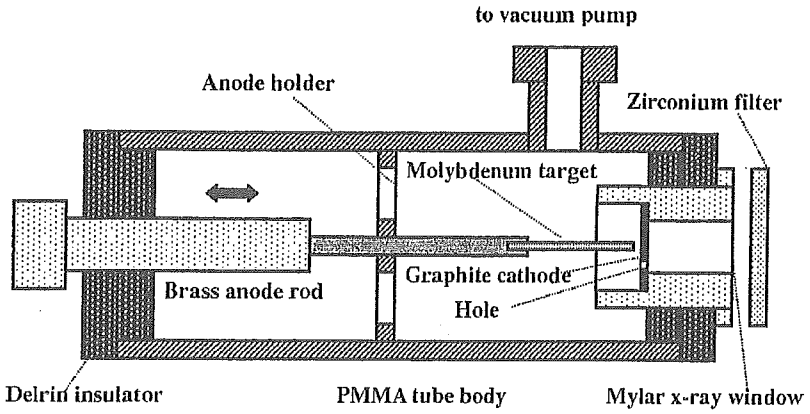

FIG. 3. Schematic drawing of the flash x-ray tube with a rod-shaped molybdenum target and a disk graphite cathode.

to approximately 0 Ω during the discharge. Thus, at the first quarter cycle of the oscillations, when the voltage decreased, the current increased. The instantaneous voltage and current increased with increases in the charging voltage, and the voltage and current were approximately 120 kV and 1.0 kA, respectively, at a charging voltage of −70 kV.

B. X-ray output

X-ray output pulse was detected using a combination of a plastic scintillator, a photomultiplier, and the filter (Fig. 6). When the charging voltage was increased, the pulse height increased, but the width seldom varied. The widths were about 70 ns, and the time-integrated x-ray dose measured by a thermoluminescence dosimeter (Kyokko TLD Reader 1500 having MSO-S elements without energy compensation) had an instantaneous value of approximately 70 μGy per pulse at 0.5 m from the x-ray source with a charging voltage of −70 kV.

C. X-ray source

In order to observe the Kα x-ray source, we employed a 100 μm-diameter pinhole camera, an x-ray film (Polaroid XR-7), and the filter (Fig. 7). When the charging voltage was increased, the spot intensity increased, and the intensities corresponded well to the x-ray pulse height. The dimension was almost equal to the target diameter and had a value of about 3.0 mm.

D. X-ray spectra

X-ray spectra were measured using a transmission-type spectrometer[11] with a lithium fluoride curved crystal 0.5 mm in thickness. The x-ray intensities of the spectra were detected by an imaging plate of a computed radiography (CR) system[15] (Konica Regius 150) with a wide dynamic range, and relative x-ray intensity was calculated from Dicom original digital data corresponding to x-ray intensity; the data was scanned by Dicom viewer in the film-less CR system. Subsequently, the relative x-ray intensity as a function of the data was calibrated using a conventional x-ray generator, and we confirmed that the intensity was proportional to the exposure time. Figure 8 shows measured spectra from the molybdenum target with the filter. In fact, we observed clean Kα lines, while bremsstrahlung rays were hardly detected at all. The Kα intensity substantially increased with increases in the charging voltage.

IV. RADIOGRAPHY

The monochromatic flash radiography was performed by the CR system at 0.5 m from the x-ray source with the filter, and the charging voltage was −70 kV.

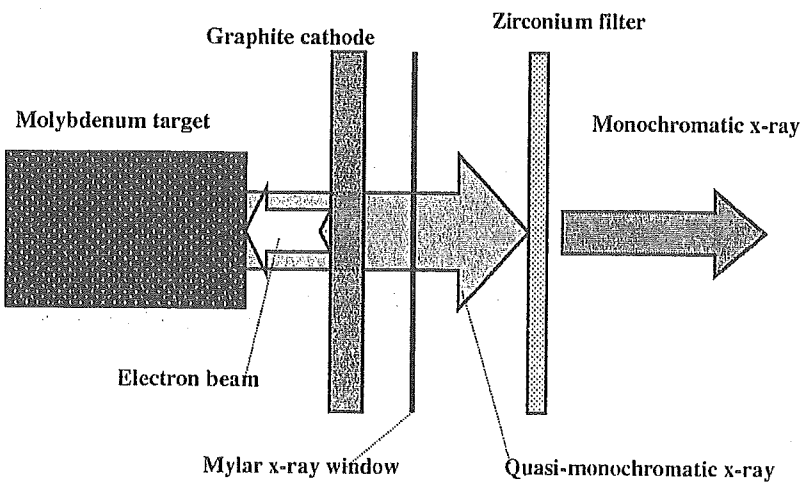

FIG. 4. Irradiation of Kα rays using a monochromatic zirconium filter. Bremsstrahlung rays are not emitted in the opposite direction to that of electron acceleration, and molybdenum Kα rays are left using a zirconium filter.

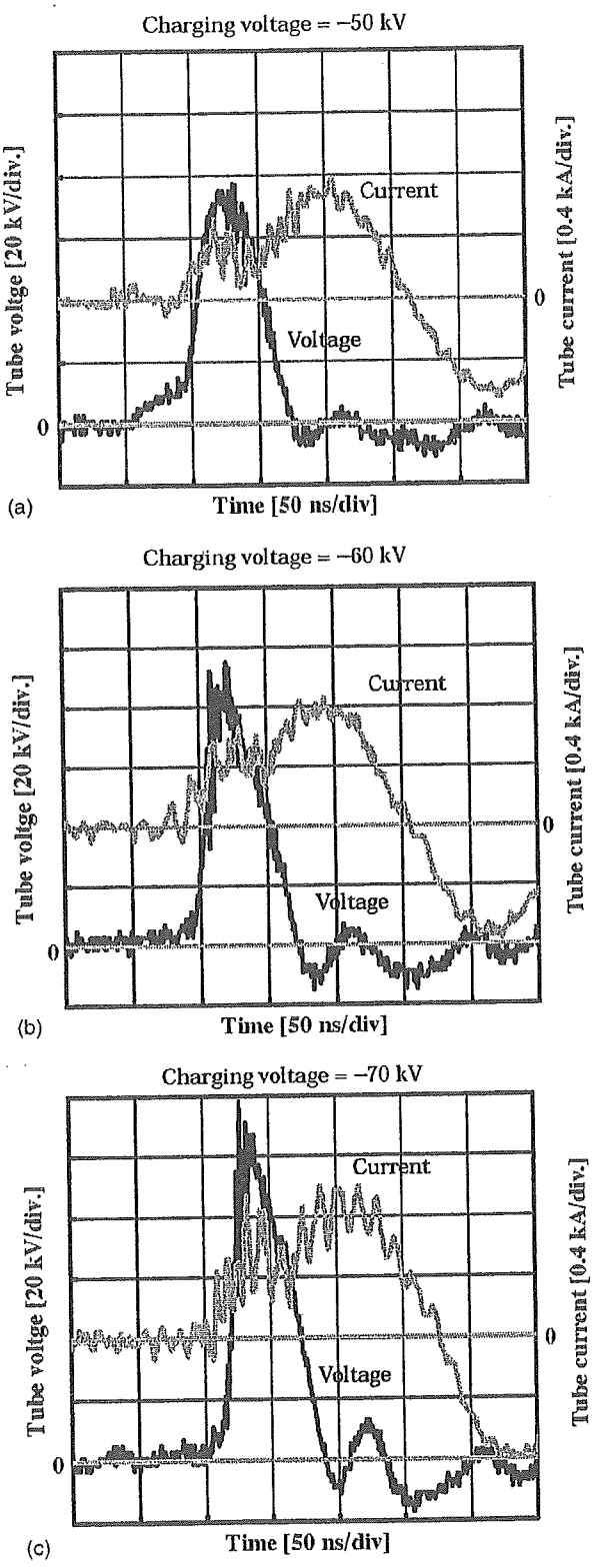

FIG. 5. Variations in the tube voltage and current with a charging voltage of (a) −50 kV, (b) −60 kV, and (c) −70 kV.

First, rough measurements of spatial resolution were made using wires. Figure 9 shows radiograms of tungsten wires coiled around a pipe made of polymethyl methacrylate. Although the image contrast increased with increases in the wire diameter, a 50 μm-diameter wire could be observed.

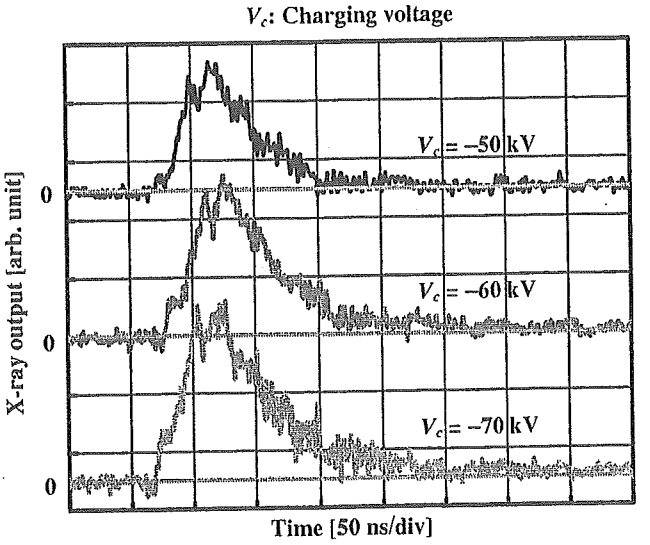

FIG. 6. X-ray outputs detected using a combination of a plastic scintillator, a photomultiplier, and the zirconium filter.

Figure 10 shows a radiogram of a vertebra, and fine structures in the vertebra were observed. Next, the image of water falling into a polypropylene beaker from a glass test tube is shown in Fig. 11. This image was taken with the slight addition of an iodine-based contrast medium. Because the x-ray duration was about 70 ns, the stop-motion image of water could be obtained. Figure 12 shows an angiogram of a rabbit heart; iodine-based microspheres of 15 μm in diameter were used, and fine blood vessels of about 100 μm were visible.

V. DISCUSSION

Concerning the spectrum measurement, we obtained fairly clean molybdenum Kα rays (17.4 keV). Therefore, we are very interested in the measurement the Kα rays from nickel (7.47 keV), copper (8.04 keV), silver (22.1 keV), cerium (34.6 keV), and tungsten (58.9 keV) targets; the target element should be selected corresponding to the radiographic objectives. In a medical application, K-series characteristic x rays of cerium are absorbed effectively by an iodine-based contrast medium with a K-edge of 33.2 keV, and high contrast microangiography can be performed.

In this research, the generator produced instantaneous number of Kα photons was approximately 3×10^7

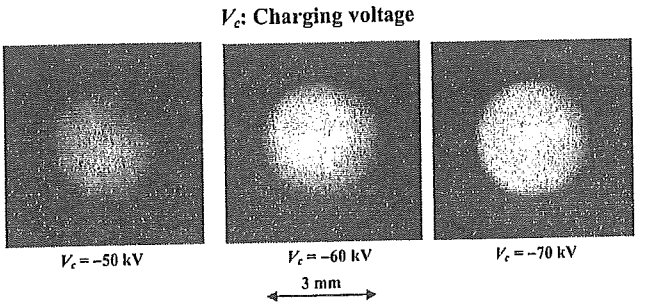

FIG. 7. Images of the x-ray source of Kα lines obtained using a pinhole camera with changes in the charging voltage.

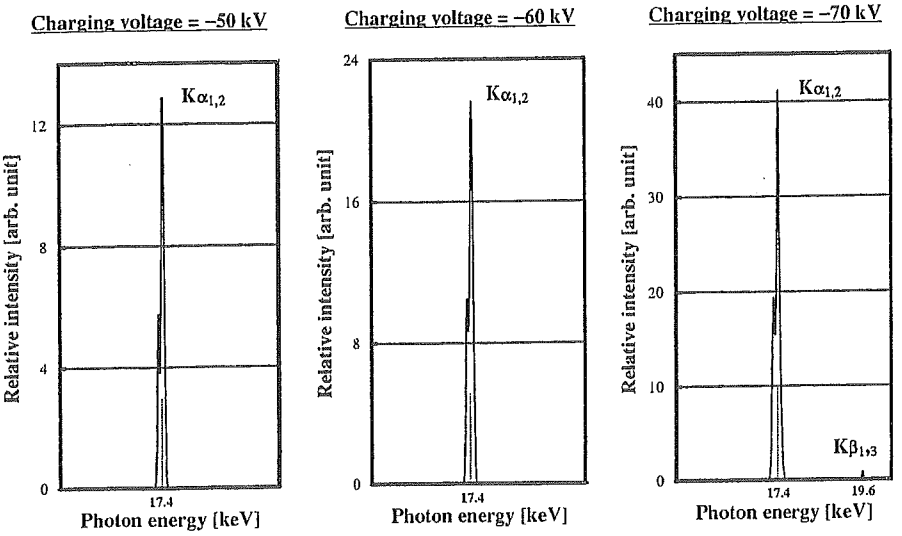

FIG. 8. X-ray spectra from the molybdenum target with the filter. The spectra were measured using a transmission type spectrometer with a lithium fluoride curved crystal.

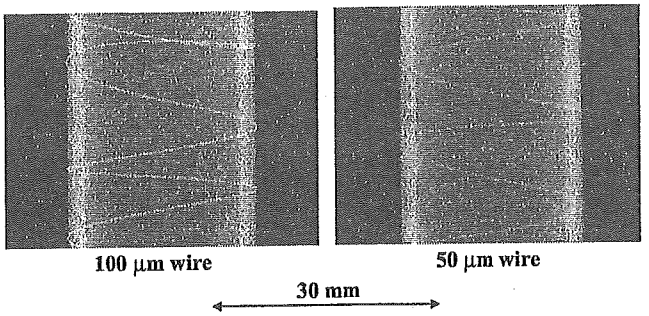

FIG. 9. Radiograms of tungsten wires of 50 and 100 μm in diameter coiled around a pipe made of polymethyl methacrylate. A 50 μm-diameter wire could be observed.

photons/cm^2 per pulse at 0.5 m from the source. Because the molybdenum plasma generator produced approximately 5 $\times 10^8$ photons/cm^2 per pulse at 1.0 m from the source, the x-ray intensity of Kα lines had a lower value as compared with the plasma x-ray generator[11] described above, which utilizes a large capacity condenser of approximately 200 nF. However, the intensity can be increased by increasing the electrostatic energy in condensers in the surge generator, and quasi-monochromatic x rays of both Kα and Kβ (19.6 keV) lines are produced without using the zirconium filter with a K-edge of 17.9 keV.

Using this flash x-ray generator, the photon energy of characteristic x rays can be selected, and we plan to design a high-speed photon-counting radiography system in order to decrease noise from radiograms. In addition, steady-state

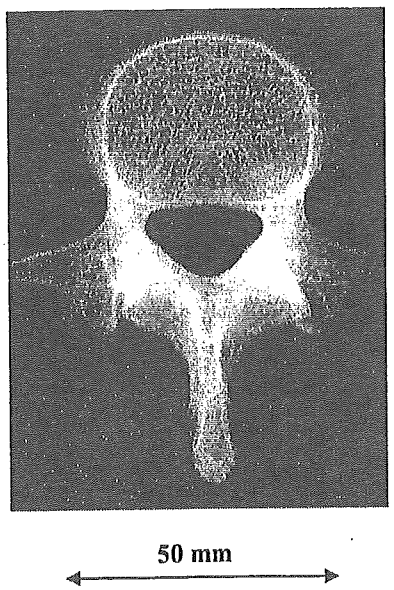

FIG. 10. Radiogram of a vertebra. Fine structure of the vertebra were visible.

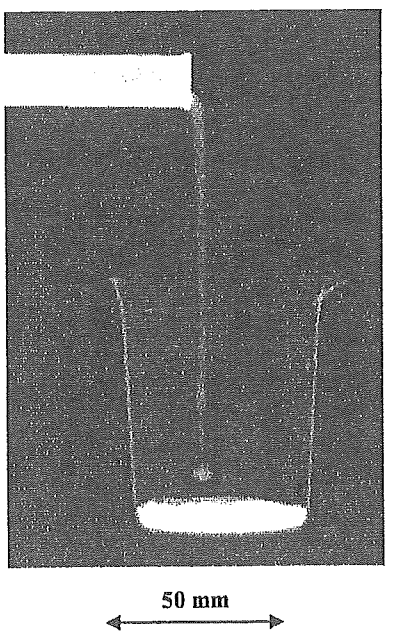

FIG. 11. Radiogram of water falling into a polypropylene beaker from a glass test tube. The stop-motion image of water was obtained by monochromatic flash radiography.

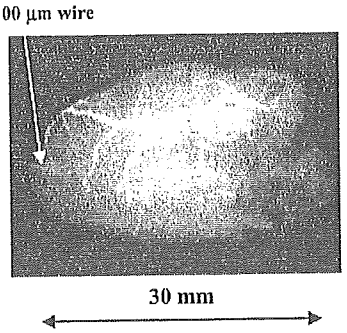

FIG. 12. Angiograms of a rabbit heart. Fine blood vessels of approximately 100 μm were visible.

monochromatic x rays for fluoroscopy can be produced by a similar tube using a constant high-voltage power supply. In conjunction with the fine focusing, these low-cost monochromatic x-ray generators will be employed to perform K-edge angiography and x-ray phase imaging for edge enhancement.[16]

ACKNOWLEDGMENTS

This work was supported by Grants-in-Aid for Scientific Research (13470154, 13877114, and 16591222) and Advanced Medical Scientific Research from MECSST, Grants from Keiryo Research Foundation, The Promotion and Mutual Aid Corporation for the Private School of Japan, JST (Test of Fostering Potential), NEDO, and MHLW (HLSRG, RAMT-nano-001, RHGTEFB-genome-005, and RGCD13C-1).

[a]Electronic mail: dresato@iwate-med.ac.jp

[1]J. J. Rocca, V. Shlyaptsev, F. G. Tomasel, O. D. Cortazar, D. Hartshorn, and J. L. A. Chilla, "Demonstration of a discharge pumped table-top soft x-ray laser," Phys. Rev. Lett. **73**, 2192–2195 (1994).

[2]J. J. Rocca, D. P. Clark, J. L. A. Chilla, and V. N. Shlyaptsev, "Energy extraction and achievement of the saturation linit in a discharge-pumped table-top soft x-ray amplifier," Phys. Rev. Lett. **77**, 1476–1479 (1996).

[3]C. D. Macchietto, B. R. Benware, and J. J. Rocca, "Generation of millijoule-level soft-x-ray laser pulses at a 4-Hz repetition rate in a highly saturated tabletop capillary discharge amplifier," Opt. Lett. **24**, 1115–1117 (1999).

[4]E. Sato, H. Isobe, and F. Hoshino, "High intensity flash x-ray apparatus for biomedical radiography," Rev. Sci. Instrum. **57**, 1399–1408 (1986).

[5]A. Shikoda, E. Sato, M. Sagae, T. Oizumi, Y. Tamakawa, and T. Yanagisawa, "Repetitive flash x-ray generator having a high-durability diode driven by a two-cable-type line pulser," Rev. Sci. Instrum. **65**, 850–856 (1994).

[6]E. Sato, K. Takahashi, M. Sagae, S. Kimura, T. Oizumi, Y. Hayasi, Y. Tamakawa, and T. Yanagisawa, "Sub-kilohertz flash x-ray generator utilizing a glass-enclosed cold-cathode triode," Med. Biol. Eng. Comput. **32**, 289–294 (1994).

[7]K. Takahashi, E. Sato, M. Sagae, T. Oizumi, Y. Tamakawa, and T. Yanagisawa, "Fundamental study on a long-duration flash x-ray generator with a surface-discharge triode," Jpn. J. Appl. Phys., Part 1 **33**, 4146–4151 (1994).

[8]E. Sato, K. Takahashi, M. Sagae, S. Kimura, T. Oizumi, Y. Hayasi, Y. Tamakawa, and T. Yanagisawa, "Sub-kilohertz flash x-ray generator utilizing a glass-enclosed cold-cathode triode," Med. Biol. Eng. Comput. **32**, 289–294 (1994).

[9]E. Sato, R. Germer, Y. Hayasi, E. Tanaka, H. Mori, T. Kawai, T. Usuki, K. Sato, H. Obara, M. Zuguchi, T. Ichimaru, H. Ojima, K. Takayama, and H. Ido, "Plasma flash x-ray generator (PFXG-02)," Proc. SPIE **4948**, 604–609 (2002).

[10]E. Sato, Y. Hayasi, R. Germer, E. Tanaka, H. Mori, T. Kwai, T. Ichimaru, K. Takayama, and Hideaki Ido, "Quasi-monochromatic flash x-ray generator utilizing weakly ionized linear copper plasma," Rev. Sci. Instrum. **74**, 5236–5240 (2003).

[11]E. Sato, Y. Hayasi, R. Germer, E. Tanaka, H. Mori, T. Kawai, H. Obara, T. Ichimaru, K. Takayama, and H. Ido, "Irradiation of intense characteristic x-rays from weakly ionized linear molybdenum plasma," Jpn. J. Med. Phys. **23**, 123–131 (2003).

[12]E. Sato, Y. Hayasi, R. Germer, E. Tanaka, H. Mori, T. Kawai, H. Obara, T. Ichimaru, K. Takayama, and H. Ido, "Intense characteristic x-ray irradiation from weakly ionized linear plasma and applications," Jpn. J. Med. Imag. Inform. Sci. **20**, 148–155 (2003).

[13]A. Mattsson, "Some characteristics of a 600 kV flash x-ray tube," Phys. Scr. **5**, 99–102 (1972).

[14]R. Germer, "X-ray flash techniques," J. Phys. E **12**, 336–350 (1979).

[15]E. Sato, K. Sato, and Y. Tamakawa, "Film-less computed radiography system for high-speed imaging," Ann. Rep. Iwate Med. Univ. Sch. Lib. Arts Sci. **35**, 13–23 (2000).

[16]A. Ishisaka, H. Ohara, and C. Honda, "A new method of analyzing edge effect in phase contrast imaging with incoherent x-rays," Opt. Rev. **7**, 566–572 (2000).

Japanese Journal of Applied Physics
Vol. 44, No. 1A, 2005, pp. 446–449

Quasi-Monochromatic X-Ray Generator Utilizing Graphite Cathode Diode with Transmission-Type Molybdenum Target

Michiaki SAGAE, Eiichi SATO, Etsuro TANAKA[1], Yasuomi HAYASI, Hidezo MORI[2], Toshiaki KAWAI[3], Toshio ICHIMARU[4], Shigehiro SATO[5], Kazuyoshi TAKAYAMA[6] and Hideaki IDO[7]

Department of Physics, Iwate Medical University, 3-16-1 Honchodori, Morioka 020-0015, Japan
[1]*Department of Nutritional Science, Faculty of Applied Bio-science, Tokyo University of Agriculture, 1-1-1 Sakuragaoka, Setagaya-ku 156-8502, Japan*
[2]*Department of Cardiac Physiology, National Cardiovascular Center Research Institute, 5-7-1 Fujishiro-dai, Suita, Osaka 565-8565, Japan*
[3]*Electron Tube Division #2, Hamamatsu Photonics K.K., 314-5 Shimokanzo, Toyooka Village, Iwata-gun 438-0193, Japan*
[4]*Department of Radiological Technology, School of Health Sciences, Hirosaki University, 66-1 Honcho, Hirosaki 036-8564, Japan*
[5]*Department of Microbiology, School of Medicine, Iwate Medical University, 19-1 Uchimaru, Morioka 020-8505, Japan*
[6]*Shock Wave Research Center, Institute of Fluid Science, Tohoku University, 2-1-1 Katahira, Aoba-ku, Sendai 980-8577, Japan*
[7]*Department of Applied Physics and Informatics, Faculty of Engineering, Tohoku Gakuin University, 1-13-1 Chuo, Tagajo 985-8537, Japan*

(Received June 19, 2004; accepted October 15, 2004; published January 11, 2005)

An X-ray generator consists of a negative high-voltage power supply and a field-emission-type cold-cathode X-ray tube. The tube is a glass-enclosed diode utilizing a transmission-type molybdenum target with a thickness of 20 μm, a needle graphite (carbon) cathode, a glass tube body, and a 0.5-mm-thick beryllium window. The tube current decreases gradually with time. After aging for 30 minutes, the tube current was approximately 0.2 mA with a tube voltage of 25 kV, and the focal-spot dimensions were 2.2 × 1.6 mm. Characteristic X-rays of molybdenum K-series were obtained after penetrating the molybdenum target and the beryllium window, and the K-absorption edge was observed clearly. The generator produced number of K photons was approximately 4×10^6 photons/cm^2·s at 1.0 m from the source. The average photon energies of Kα and Kβ lines were 17.4 and 19.6 keV, respectively, and quasi-monochromatic radiography was performed using a computed radiography system. [DOI: 10.1143/JJAP.44.446]

KEYWORDS: quasi-monochromatic X-rays, characteristic molybdenum X-rays, field emission, transmission target, quasi-monochromatic radiography

1. Introduction

Conventional medical X-ray tubes enable the observation of parts of the inside of the human body that cannot be seen by other ways. The X-ray images obtained with these tubes are exposed by both the bremsstrahlung and characteristic X-rays, unless monochromatic radiography is specifically performed. Monochromatic parallel X-ray beams are produced by synchrotrons using single crystals, and these beams have been employed to perform enhanced K-edge angiography[1–3] and X-ray phase imaging.[4,5] Subsequently, monochromatic X-ray computed tomography at two different energies has provided information on the electron density of human tissue.[6] In addition, a compact pulsed tunable monochromatic X-ray source has been designed, developed, and tested.[7] From the source, conical X-ray beams from 10 to 50 keV with pulse widths of 8 ps have been produced, and these beams are useful for biomedical imaging and protein crystallography.

Currently, flash X-ray generators[8–12] utilize cold-cathode radiation tubes and produce extremely high-dose-rate X-ray pulses with durations of less than 1 μs. In order to produce monochromatic X-rays, plasma flash X-ray generators are useful, since intense and sharp characteristic X-rays have been produced from weakly ionized linear plasmas of nickel,[13] copper[14] and molybdenum,[15] while bremsstrahlung rays are rarely detected.

In order to produce steady-state X-rays using a cold-cathode tube, the combination of the target and cathode electrodes is a very important factor. In view of the cathode, a carbon nanotube[16] is a useful field emitter and can be used as a cold cathode in an X-ray tube. Without using nanotubes, electrons can be emitted comparatively easily when lines of electric force are concentrated on a needle tip. Characteristic K-series X-rays have been obtained using a filter made of the same element as the target.

In the present research, we developed a cold-cathode X-ray tube with a needle-shaped graphite cathode, and applied it to produce characteristic molybdenum K-series X-rays by uisng a transmission target.

2. Generator

Figure 1 shows the block diagram of the X-ray generator, which consists of a negative high-voltage power supply (Model 500, −100 kV-3 mA, Pulse Electric Eng. Inc.) with dimensions of 450 × 430 × 150 mm and an X-ray tube. In the X-ray tube, the negative high voltage is applied to the cathode electrode, and the anode (target) is connected to the ground potential.

The X-ray tube is a cold-cathode diode type, as illustrated in Fig. 2. In order to perform soft radiography, including mammography, we developed a quasi-monochromatic X-ray tube with a molybdenum target. This tube consists of the following major devices: a needle-shaped graphite cathode with a tip angle of 54° and a diameter of 3.0 mm, a

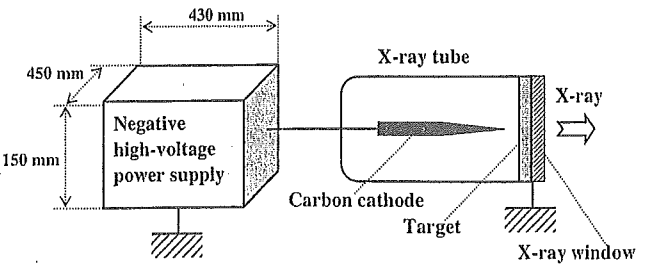

Fig. 1. Block diagram of quasi-monochromatic X-ray generator with cold-cathode diode.

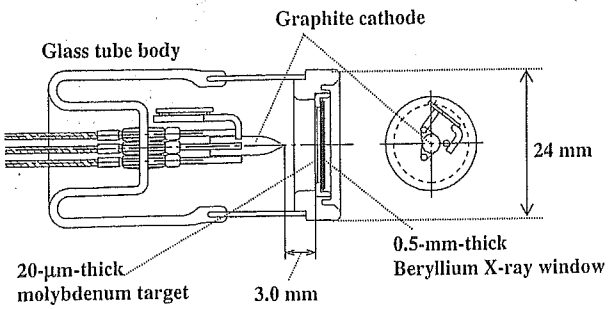

Fig. 2. Structure of X-ray tube.

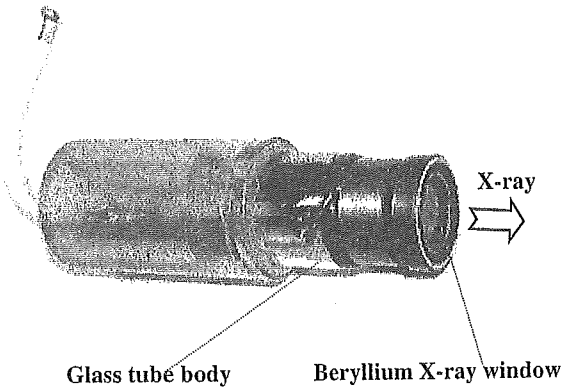

Fig. 3. Cold-cathode X-ray tube with transmission-type molybdenum target.

molybdenum disk target 20 μm thick, and a glass tube body. The target-cathode distance is 3.0 mm, and the transmission X-rays are obtained after the beam passes through the target and a 0.5-mm-thick beryllium X-ray window (Fig. 3). In this case, since the target plays the role of a K-edge filter for effectively absorbing bremsstrahlung X-rays with energies higher than the K-absorption edge, characteristic K-series X-rays are produced. The pressure in the glass-enclosed tube is primarily determined by the pressure when evacuation is stopped, and is approximately 1×10^{-4} Pa. The tube voltage is always constant and is regulated by the constant voltage power supply. Subsequently, the tube current is primarily determined by the tube voltage and the target-cathode distance, and increases with decreasing distance and increasing voltage.

In this experiment, the tube voltage applied was from 20 to 30 kV, and the exposure time was controlled in order to obtain optimum X-ray intensity for radiography.

3. Characteristics

3.1 X-ray intensity

In the field emission X-ray tube, it was very difficult to measure the X-ray intensity correctly, since the intensity gradually decreased during exposure, and small-scale vacuum breakdown may often occur. The X-ray intensity was measured using a Solidose 308 M ionization chamber for mammography at 1.0 m from the X-ray source with an exposure time of 10 s. Because the tube current increased when the tube voltage was increased, the X-ray intensity increased substantially with increasing tube voltage. In this measurement, the intensity rate with a tube voltage of 25 kV was approximately 0.3 μC/kg·s (=10 μJ/kg·s = 10 μGy/s) at 1.0 m from the source.

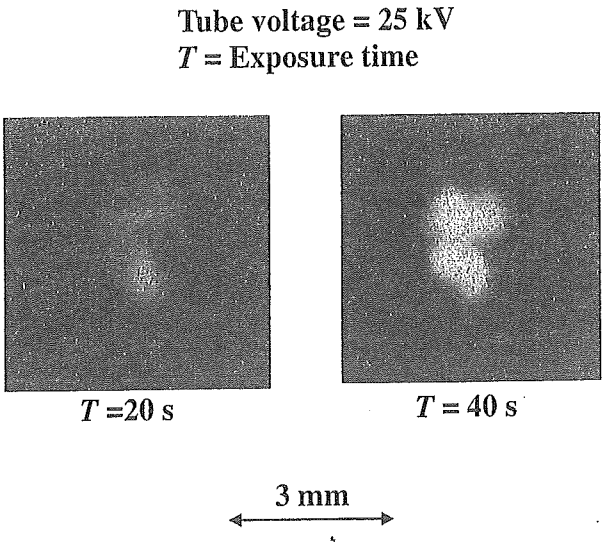

Fig. 4. Images of X-ray source with changes in exposure time.

3.2 X-ray source

In order to measure the images of the X-ray source, we employed a pinhole camera with a hole diameter of 100 μm in conjunction with a Polaroid XR-7 (film). When the exposure time was increased with a tube voltage of 25 kV, the spot intensity increased, but the spot dimensions seldom varied and had values of 2.2 × 1.6 mm (Fig. 4).

3.3 Cathode voltage and tube current

Cathode voltage and tube current were measured using a high-voltage divider and a resistor, respectively (Figs. 5 and 6). In this generator, the cathode voltage is −1 times the tube voltage, and we observed stable cathode voltages. Thereafter, the tube current increased exponentially with increasing tube voltage in a short time. In addition, the current was unstable, and decreased gradually with time.

3.4 X-ray spectra

X-ray spectra were measured using a transmission-type spectrometer with a curved lithium fluoride crystal 0.5 mm thick. The spectra were taken using a computed radiography (CR) system (Konica Regius 150)[17] with a wide dynamic range, and relative X-ray intensity was calculated from Dicom digital data. Figure 7 shows the measured spectra from the transmission-type molybdenum target. We observed lines of characteristic K-series X-rays and K-absorption edges of molybdenum. The characteristic X-ray intensity of the Kα and Kβ lines increased substantially when the tube voltage was increased.

4. Radiography

Radiography was performed using the CR system with a sampling pitch of 87.5 μm. The distance between the X-ray source and the imaging plate was 1.0 m.

Spatial resolution was roughly measured using wires. Radiograms of tungsten wires coiled around a pipe made of polymethyl methacrylate are shown in Fig. 8. Although the

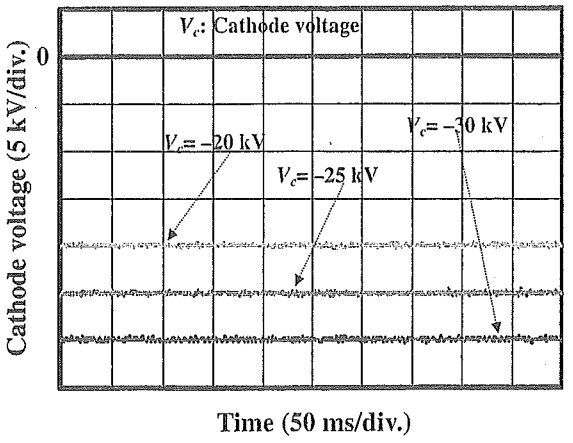

Fig. 5. Cathode voltages.

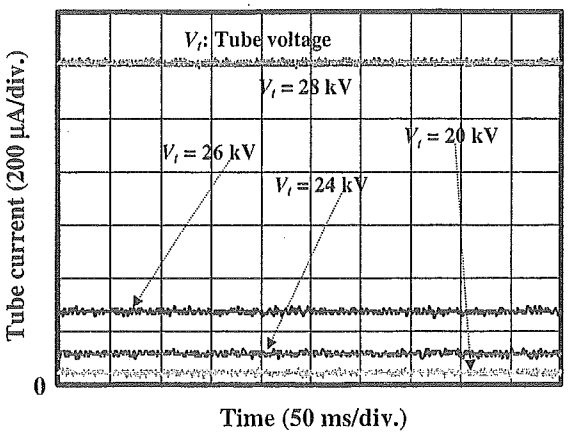

Fig. 6. Tube currents.

image contrast decreased somewhat with decreasing wire diameter due to blurring of the image caused by the sampling pitch, a 50-μm-diameter wire could be observed.

Figures 9 and 10 show angiograms of hearts. Iodine-based microspheres of 15 μm in diameter were used, and coronary

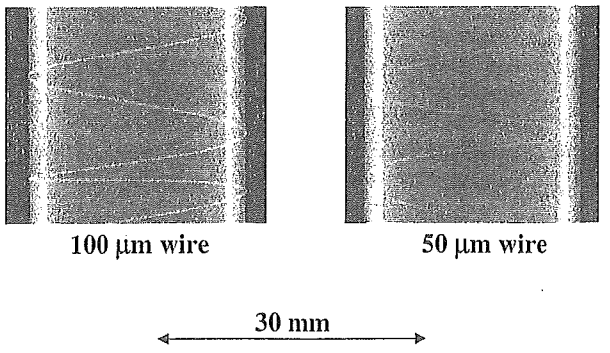

Fig. 8. Radiograms of tungsten wires of 50 and 100 μm diameter coiled around a pipe made of polymethyl methacrylate with tube voltage of 25 kV and exposure time of 20 s.

arteries and fine blood vessels of approximately 100 μm diameter were visible.

5. Discussion

In summary, we developed a simple X-ray generator with the cold-cathode diode and succeeded in producing characteristic molybdenum K-series X-rays using the transmission target as the K-edge filter. Subsequently, we confirmed the filtering effect of the target, and bremsstrahlung X-rays with photon energies higher than the edge were rarely detected with a tube voltage of 23 kV.

The current density J (A/cm^2) under field emission is written as:

$$J = 1.54 \times 10^{-6}(V/d)^2 \cdot \exp(-6.8 \times 10^7 \phi^{1.5} d/V)/\phi, \quad (1)$$

where V (V) is the tube voltage, d (cm) is the target-cathode distance, and ϕ (V) is the work function of the cathode element. Therefore, the current values in Fig. 6 corresponded qualitatively to eq. (1).

During the X-ray exposure, although the tube current decreases slightly due to ion sputtering, stable current flow can be obtained by selecting the appropriate cathode material and by controlling the radius of curvature of the cathode tip. In addition, the generator-produced number of

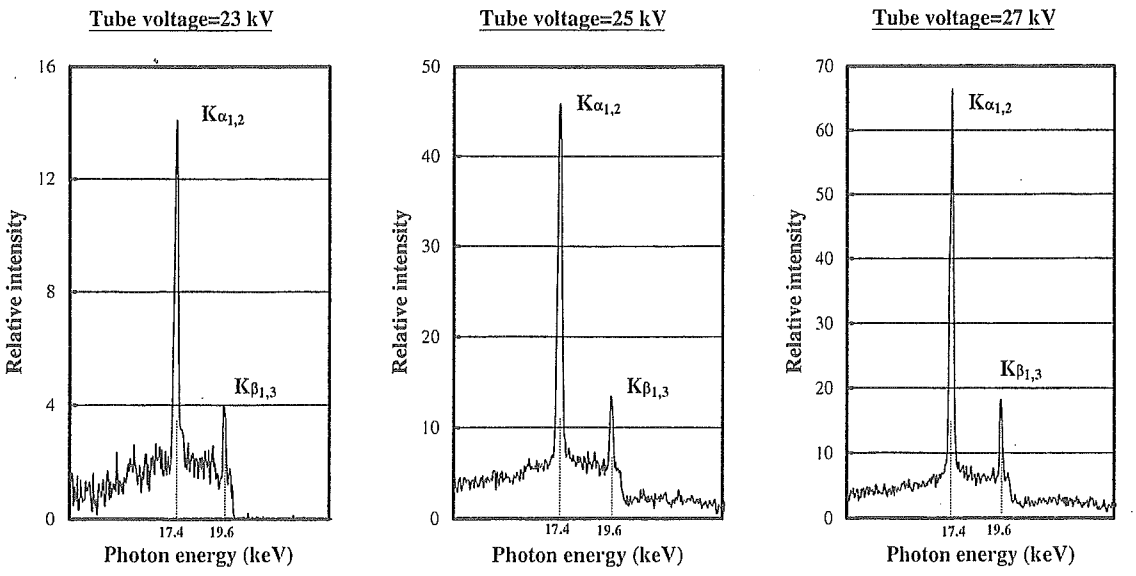

Fig. 7. X-ray spectra.

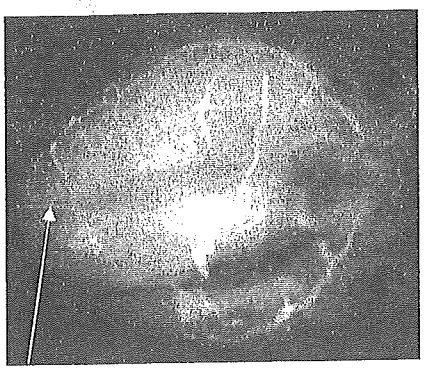

Fig. 9. Angiogram, using iodine microspheres, of extracted rabbit heart. Tube voltage and exposure time were 25 kV and 20 s, respectively.

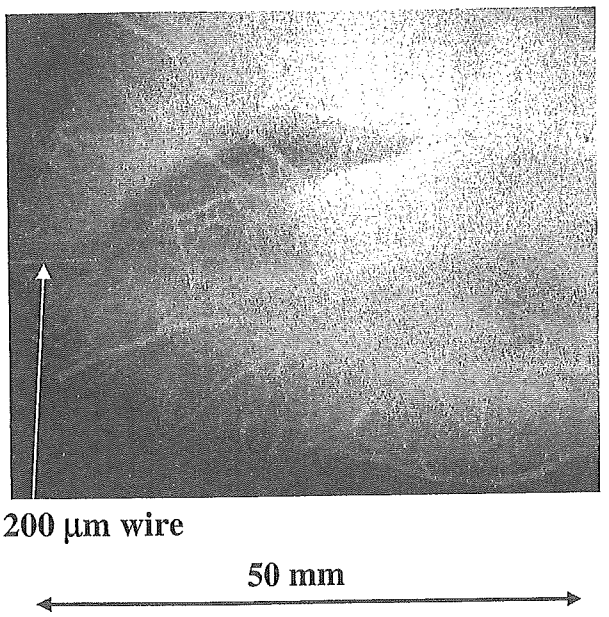

Fig. 10. Angiogram of extracted dog heart with tube voltage of 25 kV and exposure time of 60 s.

characteristic photons was approximately 4×10^6 photons/$cm^2 \cdot s$ at 1.0 m from the source with a tube voltage of 25 kV, and the photon count rate could be increased easily by increasing the tube voltage and current.

The focal spot dimensions decrease with decreasing target-cathode space, and the distance between the X-ray source and the imaging plate should be increased as much as possible to improve the spatial resolution. In soft radiography achieved with characteristic molybdenum K-series X-rays, because an X-ray lens such as a polycapillary plate[18] can be employed, the spatial resolution may be improved by decreasing the inner capillary diameter.

Under the pulsed operation, the high-voltage durability increases substantially, and both the size of the X-ray tube and the diameter of the high-voltage coaxial cable can be decreased. In this case, because the time-average tube current is regulated by the pulse repetition rate, both the tube voltage and the current can be controlled without using a hot cathode.

Recently, we developed a cerium-target X-ray tube to perform enhanced K-edge angiography utilizing cerium Kα rays (34.6 keV), since the rays are absorbed effectively by iodine-based contrast media with a K-edge of 33.2 keV. In addition, Kα rays from ytterbium (52.0 keV), tantalum (57.1 keV), and tungsten (58.9 keV) targets are very useful for performing K-edge angiography using gadolinium-based contrast media with an edge of 50.2 keV. Hence, using these rays, because the absorbed dose can be decreased effectively, extremely low-dose angiography can be accomplished.

Acknowledgment

This work was supported by Grants-in-Aid for Scientific Research (13470154, 13877114, and 16591222) and Advanced Medical Scientific Research from MECSST, Grants from Keiryo Research Foundation, The Promotion and Mutual Aid Corporation for Private Schools of Japan, JST, NEDO, and MHLW (HLSRG, RAMT-nano-001, RHGTEFB-genome-005, and RGCD13C-1).

1) A. C. Thompson, H. D. Zeman, G. S. Brown, J. Morrison, P. Reiser, V. Padmanabahn, L. Ong, S. Green, J. Giacomini, H. Gordon and E. Rubenstein: Rev. Sci. Instrum. **63** (1992) 625.
2) H. Mori *et al.*: Radiology **201** (1996) 173.
3) K. Hyodo, M. Ando, Y. Oku, S. Yamamoto, T. Takeda, Y. Itai, S. Ohtsuka, Y. Sugishita and J. Tada: J. Synchrotron Rad. **5** (1998) 1123.
4) T. J. Davis, D. Gao, T. E. Gureyev, A. W. Stevenson and S. W. Wilkims: Nature **373** (1995) 595.
5) A. Momose, T. Takeda, Y. Itai and K. Hirano: Nature Medicine **2** (1996) 473.
6) M. Torikoshi, T. Tsunoo, M. Sasaki, M. Endo, Y. Noda, T. Kohno, K. Hyodo, K. Uesugi and N. Yagi: Phys. Med. Biol. **48** (2003) 673.
7) F. E. Carroll, M. H. Mendenhall, R. H. Traeger, C. Brau and J. W. Waters: Am. J. Roentgenol. **181** (2003) 1197.
8) R. Germer: J. Phys. E: Sci. Instrum. **12** (1979) 336.
9) E. Sato, H. Isobe and F. Hoshino: Rev. Sci. Instrum. **57** (1986) 1399.
10) A. Shikoda, E. Sato, M. Sagae, T. Oizumi, Y. Tamakawa and T. Yanagisawa: Rev. Sci. Instrum. **65** (1994) 850.
11) K. Takahashi, E. Sato, M. Sagae, T. Oizumi, Y. Tamakawa and T. Yanagisawa: Jpn. J. Appl. Phys. **33** (1994) 4146.
12) E. Sato, K. Takahashi, M. Sagae, S. Kimura, T. Oizumi, Y. Hayasi, Y. Tamakawa and T. Yanagisawa: Med. & Biol. Eng. & Comput. **32** (1994) 289.
13) E. Sato, Y. Hayasi, R. Germer, E. Tanaka, H. Mori, T. Kawai, T. Ichimaru, S. Sato, K. Takayama and H. Ido: J. Electron Spectrosc. & Related Phenom. **137–140** (2004) 713.
14) E. Sato, Y. Hayasi, R. Germer, E. Tanaka, H. Mori, T. Kawai, T. Ichimaru, K. Takayama and H. Ido: Rev. Sci. Instrum. **74** (2003) 5236.
15) E. Sato, Y. Hayasi, R. Germer, E. Tanaka, H. Mori, T. Kawai, H. Obara, T. Ichimaru, K. Takayama and H. Ido: Jpn. J. Med. Phys. **20** (2003) 123.
16) H. Sugie, M. Tanemura, V. Filip, K. Iwata, K. Takahashi and F. Okuyama: Appl. Phys. Lett. **78** (2000) 2578.
17) E. Sato, K. Sato and Y. Tamakawa: Ann. Rep. Iwate Med. Univ. Sch. Lib. Arts Sci. **35** (2000) 13.
18) E. Sato, Y. Hayasi, R. Germer, E. Tanaka, H. Mori, T. Kawai, T. Ichimaru, S. Sato, K. Takayama and H. Ido: J. Electron Spectrosc. Related Phenom. **137–140** (2004) 705.

ELSEVIER

Cardiovascular Research 65 (2005) 334–344

Cardiovascular Research

www.elsevier.com/locate/cardiores

Purified cardiomyocytes from bone marrow mesenchymal stem cells produce stable intracardiac grafts in mice

Naoichiro Hattan[a,1], Haruko Kawaguchi[b,1], Kiyoshi Ando[c], Eriko Kuwabara[a], Jun Fujita[d], Mitsushige Murata[d], Makoto Suematsu[b], Hidezo Mori[a], Keiichi Fukuda[d,*]

[a]*Department of Physiology, Tokai University School of Medicine, Japan*
[b]*Department of Biochemistry and Integrative Medical Biology, Keio University School of Medicine, Tokyo, Japan*
[c]*Department of Hematology and Oncology, Tokai University School of Medicine, Japan*
[d]*Department of Medicine, Division of Cardiology, Keio University School of Medicine, 35 Shinanomachi, Shinjuku-ku, Tokyo 160-8582, Japan*

Received 16 April 2004; received in revised form 4 October 2004; accepted 5 October 2004
Available online 28 October 2004
Time for primary review 21 days

Abstract

Objective: We have previously isolated cardiomyogenic cells from murine bone marrow (CMG cells). Regenerated cardiomyocytes are important candidates for cell transplantation, but as they are stem cell derived, they can be contaminated with various cell types, thereby requiring characterization and purification. Our objectives were to increase the efficiency of cell transplantation and to protect the recipients from possible adverse effects using an efficient and effective purification process as well as to characterize regenerated cardiomyocytes.
Methods: Noncardiomyocytes were eliminated from a mixture of stem-cell-derived cells using a fluorescence-activated cell sorter to specifically isolate CMG cells transfected with a recombinant plasmid containing enhanced green fluorescent protein (EGFP) cDNA under the control of the myosin light chain-2v (MLC-2v) promoter. Gene expression and the action potential were investigated, and purified cells were transplanted into the heart of adult mice.
Results: Six percent to 24% of transfected CMG cells expressed EGFP after differentiation was induced, and a strong EGFP-positive fraction was selected. All the sorted cells began spontaneous beating after 3 weeks. These cells expressed cardiomyocyte-specific genes such as α-skeletal actin, β-myosin heavy chain, MLC-2v, and CaV1.2 and incorporated bromodeoxyuridine for 5 days. The isolated EGFP-positive cells were expanded for 5 days and then transplanted into the left ventricle of adult mouse hearts. The transplanted cells survived for at least 3 months and were oriented in parallel to the cardiomyocytes of the recipient heart.
Conclusions: The purification and transplantation of differentiated cardiomyocytes from adult stem cells provides a viable model of tissue engineering for the treatment of heart failure.

Keywords: Cardiomyocytes; Heart failure; Transplantation; Stem cell; Bone marrow

This article is referred to in the Editorial by B. Dawn and R. Bolli (pages 293–295) in this issue.

1. Introduction

Necrotic cardiomyocytes in infarcted ventricular tissue are progressively replaced by fibroblasts leading to the formation of scar tissue and this loss of cardiomyocytes leads to regional contractile dysfunction. Transplanted fetal cardiomyocytes can survive in heart scar tissue, thereby limiting scar expansion and preventing post-infarction heart failure [1–3]. The transplantation of cultured cardiomyocytes into damaged myocardium has been proposed as a novel method

* Corresponding author. Tel.: +81 3 5363 3874; fax: +81 3 5363 3875.
E-mail address: kfukuda@sc.itc.keio.ac.jp (K. Fukuda).
[1] Naoichiro Hattan and Haruko Kawaguchi contributed equally to this paper.

0008-6363/$ - see front matter © 2004 European Society of Cardiology. Published by Elsevier B.V. All rights reserved.
doi:10.1016/j.cardiores.2004.10.004

for treating heart failure. While this is a revolutionary idea, it remains clinically unfeasible due to the difficulty in obtaining donor fetal hearts. For this reason, research has focused on the development of a cardiomyogenic cell line to treat heart failure by transplantation therapy.

Advances in regenerative medicine have enabled the generation of various cell types from embryonic stem (ES) cells or adult stem cells [4,5]. We recently reported the generation of cardiomyocytes from marrow mesenchymal stem cells in vitro (CMG cells) and demonstrated that these cells spontaneously beat, express atrial natriuretic factors, and possess a fetal ventricular cardiomyocyte-like phenotype [6]. We also reported that cardiomyocytes regenerated from marrow mesenchymal stem cells express α_{1A}, α_{1B}, α_{1D}, β_1, and β_2 adrenergic receptors and M_1 and M_2 muscarinic receptors [7]. Stimulation of the α_1 receptors with phenylephrine caused cardiomyocyte hypertrophy, and stimulation of the β receptors with isoproterenol increased the beating rate and contractility of the regenerated cardiomyocytes. These findings demonstrate the suitability of bone-marrow-derived regenerated cardiomyocytes as a candidate for use in cell transplantation therapy.

Purification of regenerated cardiomyocytes is required prior to use for cardiomyocyte transplantation. The population of cardiomyocytes in ES-cell-derived embryoid bodies is less than 10%, and the population of cardiomyocytes in 5-azacytidine-exposed CMG cells is less than 10–30%. To increase the efficiency of transplantation and protect recipients from possible adverse effects, regenerated cardiomyocytes need to be purified from the population of differentiated cell types prior to cell transplantation. Klug [8] and Muller [9] independently reported that embryonic stem-cell-derived cardiomyocytes could be purified using a cardiomyocyte-specific gene promoter–drug-resistant gene expression system. In this study, we purified bone-marrow-derived cardiomyocytes using a recombinant plasmid containing enhanced green fluorescent protein (EGFP) cDNA under the control of the myosin light chain-2v (MLC-2v) promoter. Purified cells were then transplanted into recipient mice hearts and the success of transplantation was analyzed histologically.

2. Methods

All experimental procedures and protocols were approved by the Animal Care and Use Committees of the Keio University, Japan, and the investigation conforms to the Guide for the Care and Use of Laboratory Animals published by the US National Institutes of Health (NIH Publication No. 85–23 revised 1996).

2.1. Preparation of bone marrow-derived regenerated cardiomyocytes

Murine bone-marrow-derived mesenchymal stem cells (CMG cells) were cultured in Iscove's modified Dulbecco's medium (IMDM) supplemented with 20% FBS as previously described [6,7]. The cells were exposed to 3 μmol/l of 5-azacytidine for 24 h to induce cell differentiation [6].

2.2. Construction of myosin light chain 2v-promoted EGFP plasmid

An expression vector, pMLC2v-EGFP, was constructed by cloning a 2.7-kb *Hin*dIII–*Eco*RI fragment of the rat MLC-2v promoter region [10,11] into the *Hin*dIII–*Eco*RI site of pEGFP-1 (Clontech, Palo Alto, CA), so that EGFP would be expressed under the control of MLC-2v promoter (Fig. 1a). This plasmid also contains the neomycin-resistance gene to enable selection of permanently transfected clones. MLC-2v is specifically expressed in ventricular cardiomyocytes.

2.3. Transfection of MLC2v-EGFP expression plasmid and cell selection

The MLC2v-EGFP plasmid was transfected into CMG cells by liposomal transfection. After 24 h when cells are about 20% confluent, a mixture containing 2 μg of plasmid DNA and 4 μl of LT1 TransIT Polyamine Transfection Reagent (Mirus Corporation) in OPTI-MEM (Life Technologies, Gaithersburg, MD) were added to each 35-mm culture dish. After selection with 1000 μg/ml of G418 for 4 weeks, stably transfected colonies derived from single cells were cloned and pooled. EGFP fluorescence was observed under a fluorescence microscope (Olympus TMD300, Tokyo, Japan).

2.4. Flow cytometry and cell sorting

Flow cytometry and sorting of EGFP(+) cells were performed on a FACS Vantage (Becton Dickinson, Cockeysville, MD). Cells were analyzed by light forward and side scatter and for EGFP fluorescence through a 530 nm band pass filter as they traversed the beam of an argon ion laser (488 nm, 100 mW). Nontransfected control cells were used to set the background fluorescence. Cell sorting was performed 3 days after 5-azacytidine exposure at 500 cells/s as EGFP(+) cells displaying fluorescence higher than the background level were observed at this time point.

2.5. Infection of recombinant adenovirus vectors

Replication-deficient recombinant adenovirus vector, pAdex-LacZ, was constructed by cloning LacZ cDNA into the *Swa*I site of pAdex1CAwt as previously described [12]. In this vector, *E. coli* β-galactosidase is expressed under the control of a strong, ubiquitously expressed, promoter-derived from the cytomegalovirus enhancer-chicken β-actin hybrid [13]. On day 3 after seeding, EGFP(+) cells isolated by FACS were incubated

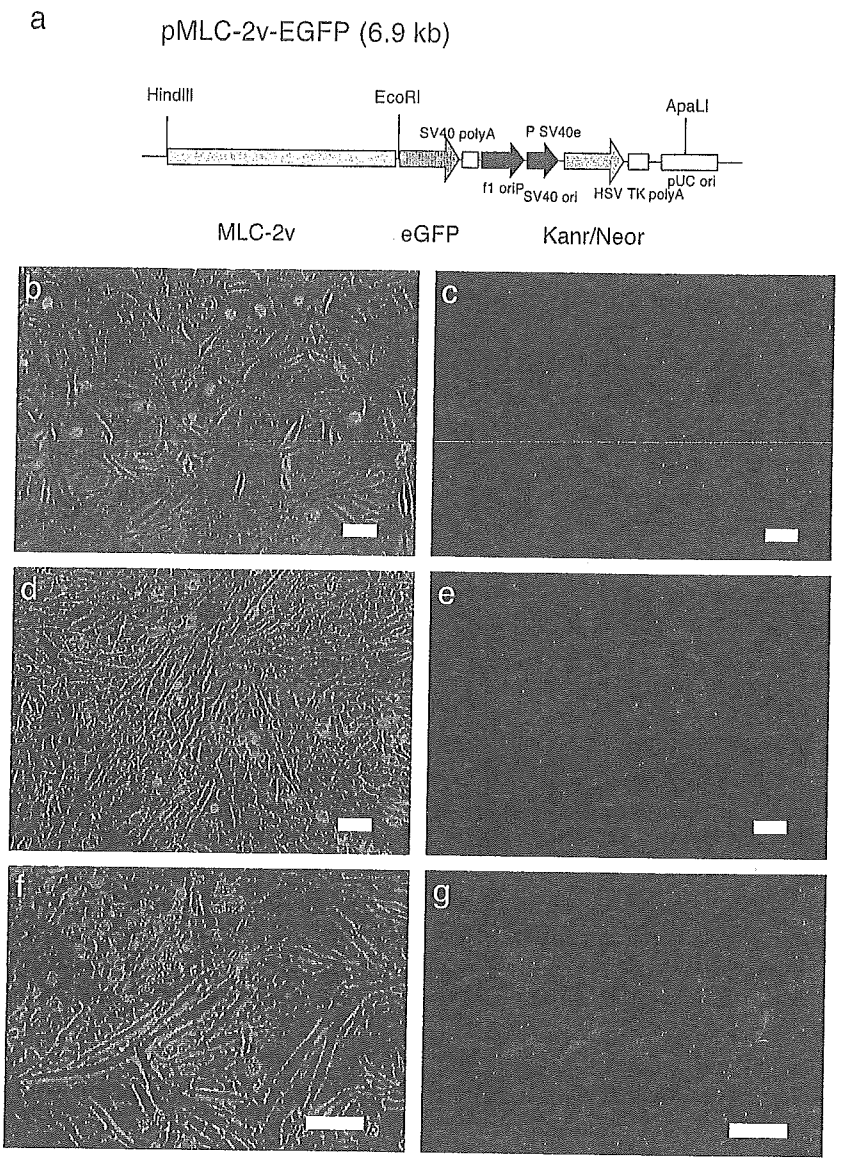

Fig. 1. Construction of pMLC-2v-EGFP and expression of EGFP in differentiated CMG cells. (a) Restriction map of pMLC-2v-EGFP. (b–g) Microscopy of the pMLC-2v-EGFP stably transfected CMG cells. b, d, and f shows phase contrast microscopy of the CMG cells after differentiation, and c, e, and g represent fluorescent microscopic views of the same field in b, d, and f. (b, c) 3 days, (d, e) 7 days, and (f, g) 4 weeks after the 5-azacytidine exposure. Bars indicate 100 μm.

with PBS containing Adex-LacZ virus at 10 MOI for 100 min. The cells were washed three times to remove virus remaining on the cell surface. Prior to transplantation, the cells were incubated in IMDM with 20% FBS for 2 days.

2.6. Transmission electron microscopy

Cells were washed three times with PBS (pH 7.4) prior to transmission electron microscopy. Cells were initially fixed with PBS containing 2.5% glutaraldehyde for 2 h. The cells were then embedded in epoxy resin. Ultra-thin sections cut horizontally to the growing surface were double stained in uranyl acetate and lead citrate, and viewed under a JEM-1200EX transmission electron microscope.

2.7. Bromodeoxyuridine (BrdU) incorporation

To detect nuclei undergoing DNA synthesis, cells were incubated with BrdU (10 μM) for 5 h, rinsed with PBS, and then fixed in methanol for 20 min at 4 °C. Immunofluorescence microscopy using a monoclonal antibody against BrdU was performed as described previously [14]. The percentage of BrdU-positive cells was estimated by counting cells on photographs of randomly chosen fields.

2.8. Gene expression analysis

Total RNA was extracted from EGFP(+) cells isolated at 7 days following transfection. RT-PCR was performed to detect α-myosin heavy chain (MHC), β-MHC, α-

skeletal actin, α-cardiac actin, myosin light chain-2v (MLC-2v), MLC-2a, Cav1.2, myoD, calponin, and α-smooth muscle actin genes. The primers and PCR cycles used were as described previously [6,15,16]. Primers for Cav1.2 were CTGCAGGTGATGATGAGGTC for the forward primer and GCGGTGTTGTTGGCGTTGTT for the reverse primer.

2.9. Immunostaining

Cells were attached to gelatin-coated glass slides, fixed in 4% paraformaldehyde, and then stained with primary antibodies against anti-GATA4, anti-troponin I, and anti-MEF2C antibodies (all from Santa Cruz Biotechnology), or anti-connexin43 antibody (Sigma). Anti-goat-IgG conjugated with Texas red or anti-rabbit IgG conjugated with Rhodamine (1:500, Pharmingen) was use as a secondary antibody.

2.10. Action potential recording

Electrophysiological studies were performed in IMDM containing (mmol/L) $CaCl_2$ 1.49, KCl 4.23, and HEPES 25 (pH 7.4). Cultured cells were placed on the stage of an inverted phase contrast optic (Diaphoto-300, Nikon) at 23 °C. Action potentials were recorded using conventional microelectrodes as described previously [8]. Intracellular recordings were taken from MLC2v-EGFP-purified cells 3 weeks following transfection.

2.11. Cell transplantation

Animal Care and Use Committees of Keio University approved all experimental procedures and protocols. Female scid mice (12 weeks) were anesthetized initially with ether and placed on a warm pad maintained at 37 °C. The trachea was cannulated with a polyethylene tube connected to a respirator (Shinano, Tokyo, Japan) with a tidal volume set at 0.6 ml and a rate set at 110/min. Mice were then anesthetized with 0.5–1.5% isoflurene under controlled ventilation with a respirator for the remainder of the surgical procedure. A left thoracotomy was performed between ribs 4 and 5, and the pericardial sac was removed. Isolated EGFP(+) cells that had been expanded for 5 days were resuspended in PBS at a concentration of 5×10^7 cells/ml. A total cell suspension volume of 50 μl was drawn into a 50 μl Hamilton syringe with a 31-gauge needle, and 10 μl was injected into the anterior wall of the left ventricle. Following the transplantation, residual cells in the syringe were collected and stained with trypan blue. The total and living cell numbers were counted. The number of living cells to inject was calculated by the following formula. (The injected living cells)=[(Total injected cells)−(Residual cells in the syringe)](Percent of living cells). Injection of PBS was used as a control.

2.12. Histological studies

The mice were sacrificed, and the hearts were dissected and fixed in 2% formaldehyde and 0.2% glutaraldehyde in PBS at room temperature for 5 min. The hearts were then washed in PBS and then incubated overnight in X-gal solution (1 mg/ml X-gal, 15 mmol/L potassium ferricyanide, 15 mmol/L potassium ferrocyanide, and 2 mmol/L $MgCl_2$ in PBS). The hearts were refixed in the same fix solution, embedded in paraffin, and sectioned into 6-μm-thick slices for hematoxylin–eosin staining. The numbers of X-gal-stained CMG cells were counted using serial sections of the transplanted heart (more than 200 slices/mouse), and an estimate of total transplanted cell survival was obtained using the following formula. (Percent of cells surviving in the recipient heart)=[(Total surviving cells in the recipient heart)/(Injected living cells)]100.

To observe EGFP fluorescence, the hearts were embedded in OCT compound and frozen with liquid nitrogen. A cryostat was used to generate 6-μm-thick sections. The samples were examined with a confocal LASER microscope (LSM510; Carl Zeiss, Jena, Germany). The GFP signal was confirmed by emission finger printing, using the LSM 510 Meta spectrometer (Carl Zeiss).

2.13. Electrocardiography (ECG) recording

ECG recordings were performed 2 and 4 weeks after transplantation. Mice were anesthetized with ether, needle limb leads were fixed, and the ECG was recorded for 1 h.

2.14. Statistics

Values are presented as mean±SD. The significance of differences among mean values was determined by ANOVA. Statistical comparison of the control and treated groups was carried out using the nonparametric Fisher's multiple comparison tests. The level accepted for significance was $p<0.05$.

3. Results

3.1. Regenerated cardiomyocytes, but not other cell types, express EGFP

G418-resistant cells were exposed to 5-azacytidine and after 3 days EGFP(+) cells exhibited a fibroblast-like morphology (Fig. 1b,c), and were difficult to distinguish from other cell types. After 7 days, the EGFP(+) cells displayed a spindle-like morphology (Fig. 1d,e), but did not spontaneously beat at this stage. After 3 weeks, the EGFP(+) cells began to appear more rod-like and form inter-cell connections and after 4 weeks spontaneous beating was observed (Fig. 1f,g). Some fractions of the EGFP(−)

cells differentiated into adipocytes, but other EGFP(−) cells did not display any specific morphology. These findings indicate that the MLC2v–EGFP system may be a useful method for distinguishing regenerated cardiomyocytes from other cell types at an early stage.

3.2. Fluorescence-activated cell sorting (FACS) analysis

FACS analysis was performed 3 day after 5-azacytidine exposure to isolate regenerated cardiomyocytes. Control cells (before 5-azacytidine exposure) showed no detectable fluorescence (Fig. 2a), whereas 3 days after 5-azacytidine exposure the cells stable transfected with the MLC2v-EGFP expression plasmid generated sufficient EGFP signal for cell sorting (Fig. 2b). The EGFP(+) fraction ranged from 6–24%. Fig. 2c,d shows the cells 4 days after cell sorting (7 days after 5-azacytidine exposure) displaying a fibroblast-like morphology. The percentage of EGFP-positive cells was calculated by comparing cell counts from phase contrast microscopy with EGFP(+) cell counts using fluorescence microscopy, 3 days after cell sorting. More than 99% of the sorted cells expressed EGFP fluorescence. After 3 weeks, these cells had a spindle-like appearance and began spontaneous beating (Fig. 2e,f).

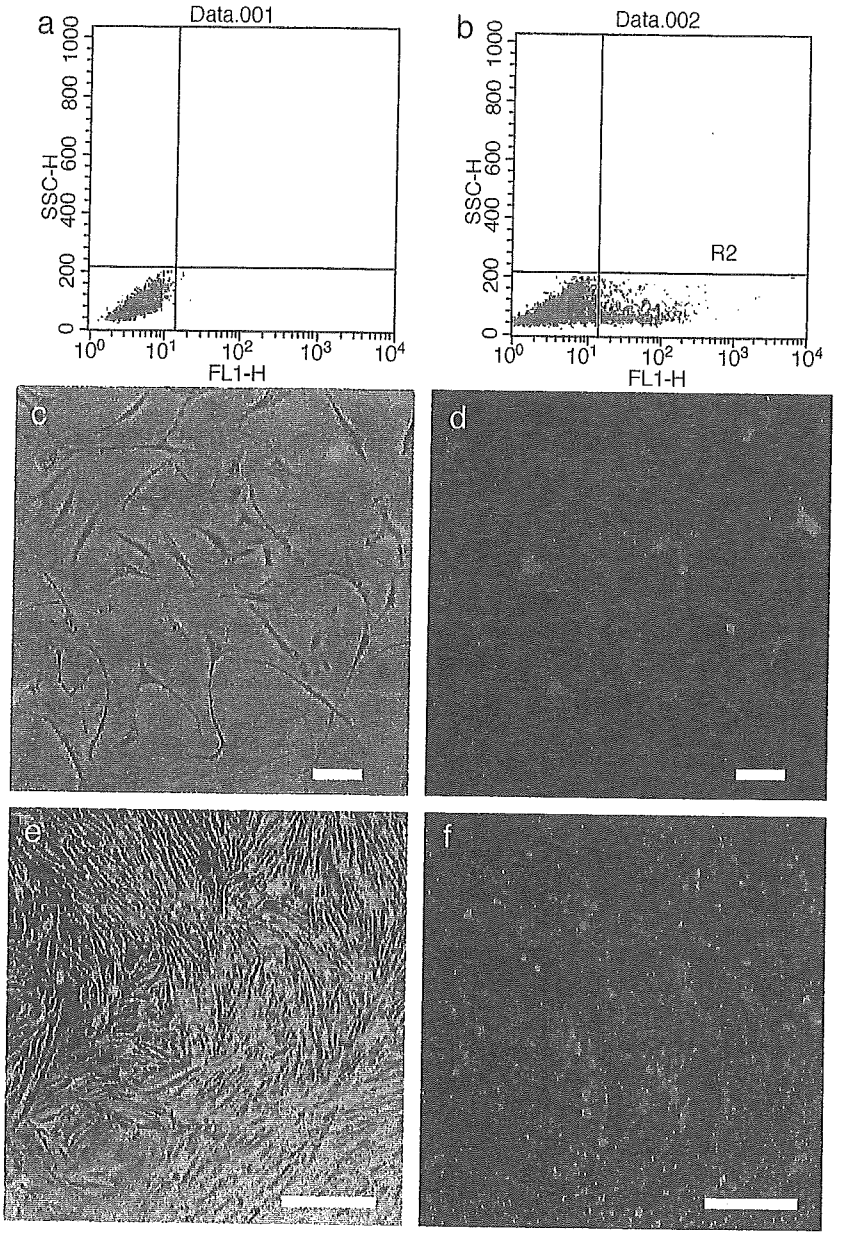

Fig. 2. FACS analysis of the pMLC-2v-EGFP-transfected cells and microscopy of the sorted cells. (a, b) FACS analysis of the pMLC-2v-EGFP-transfected cells. The horizontal axis indicates the intensity of EGFP fluorescence. (a) Control cells, (b) cells 3 days after exposure to 5-azacytidine exposure. d and f are fluorescence microscopy images of the EGFP signal. c and e are phase contrast microscopy views of the same field. (c, d) 4 days, and (e, f) 3 weeks after cell sorting. Note that all the cells display EGFP fluorescence, and that the EGFP(+) CMG cells exhibit a cardiomyocyte-like appearance and spontaneously beat after 3 weeks. Bars in c,d and e,f indicate 100 and 500 μm, respectively.